JGP Journal of General Physiology

RESEARCH ARTICLE

Pore- and voltage sensor–targeted KCNQ openers have distinct state-dependent actions

Caroline K. Wang, Shawn M. Lamothe, Alice W. Wang, Runying Y. Yang, and Harley T. Kurata

Ion channels encoded by *KCNQ2-5* generate a prominent K^+ conductance in the central nervous system, referred to as the M current, which is controlled by membrane voltage and PIP2. The KCNQ2-5 voltage-gated potassium channels are targeted by a variety of activating compounds that cause negative shifts in the voltage dependence of activation. The underlying pharmacology of these effects is of growing interest because of possible clinical applications. Recent studies have revealed multiple binding sites and mechanisms of action of KCNQ activators. For example, retigabine targets the pore domain, but several compounds have been shown to influence the voltage-sensing domain. An important unexplored feature of these compounds is the influence of channel gating on drug binding or effects. In the present study, we compare the state-dependent actions of retigabine and ICA-069673 (ICA73, a voltage sensor–targeted activator). We assess drug binding to preopen states by applying drugs to homomeric KCNQ2 channels at different holding voltages, demonstrating little or no association of ICA73 with resting states. Using rapid solution switching, we also demonstrate that the rate of onset of ICA73 correlates with the voltage dependence of channel activation. Retigabine actions differ significantly, with prominent drug effects seen at very negative holding voltages and distinct voltage dependences of drug binding versus channel activation. Using similar approaches, we investigate the mechanistic basis for attenuation of ICA73 actions by the voltage-sensing domain mutation KCNQ2[A181P]. Our findings demonstrate different state-dependent actions of pore- versus voltage sensor–targeted KCNQ channel activators, which highlight that subtypes of this drug class operate with distinct mechanisms.

Introduction

Voltage-gated potassium channels in the KCNQ (Kv7) family encode the M current, a prominent neuronal potassium current with dual regulation by voltage and PIP2 (Suh et al., 2006; Suh and Hille, 2007). The M current was first named because of its identification as a potassium current that was inhibited by extracellular ligands of muscarinic acetylcholine receptors, although these currents are now recognized as important regulators of neuronal excitability in response to a variety of extracellular signals (Adams and Brown, 1980; Brown and Adams, 1980; Brown et al., 2007; Hernandez et al., 2008). The KCNQ channels also have unique pharmacological properties, highlighted by their susceptibility to activation by an emerging class of voltage-gated potassium channel openers (Barrese et al., 2018; Miceli et al., 2018). The prototype drug in this class, retigabine, causes a hyperpolarizing shift of the voltage dependence of activation of channels that contain KCNQ2-5 subtypes, and this effect depends on the presence of a conserved Trp residue (Trp 236 in KCNQ2) in retigabine sensitive KCNQ channels (Schenzer et al., 2005; Wuttke et al., 2005; Lange et al., 2009; Kim et al., 2015).

The primary clinical application of KCNQ channel activators has been the treatment of pharmacoresistant epilepsy, and this is partly related to the recognition that KCNQ2 and KCNQ3 are associated with inheritable forms of epilepsy, varying in severity from benign familial neonatal seizures to epileptic encephalopathy (Biervert et al., 1998; Charlier et al., 1998; Singh et al., 1998; Martyn-St James et al., 2012). Mutations in KCNQ4 channels have also been linked to age-related deafness (Kubisch et al., 1999; Kharkovets et al., 2006). In addition to utility in epilepsy, applications for treatment of tinnitus, hypertension, pain, and neurodegenerative diseases are also being explored (Mackie and Byron, 2008; Xu et al., 2010; Wainger et al., 2014; Kalappa et al., 2015; Kumar et al., 2016; Vicente-Baz et al., 2016). Production of retigabine was recently discontinued because of low usage and some undesirable side effects including urinary retention and localized blue pigmentation in some patients. However, the identifi-

Department of Pharmacology, Alberta Diabetes Institute, University of Alberta, Edmonton, Alberta, Canada.

Correspondence to Harley T. Kurata: kurata@ualberta.ca.

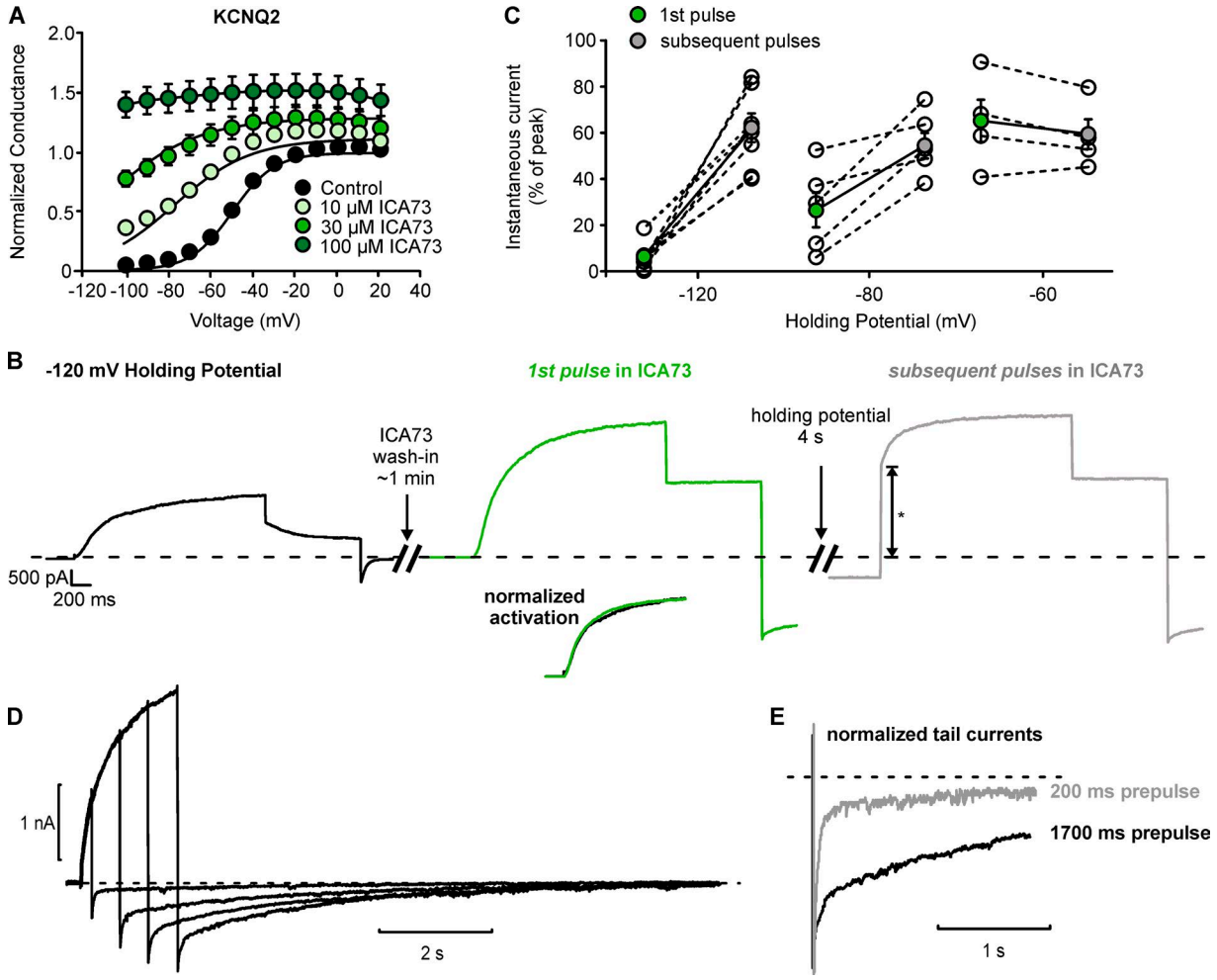

Figure 1. **The ICA73 is excluded from resting KCNQ2 channels. (A)** Conductance–voltage relationships for WT KCNQ2 channels expressed in *Xenopus laevis* oocytes in various concentrations of ICA73, normalized to peak current in control for each cell. The KCNQ2 gating parameters were as follows: control $V_{1/2}$ = −48.7 ± 1.0 mV, k = 9.9 ± 0.4 mV; 10 µM ICA73 $V_{1/2}$ = −76.4 ± 2.2 mV, k = 17.9 ± 0.5 mV; and 30 µM ICA73 $V_{1/2}$ = −108.6 ± 3.0 mV, k = 21.3 ± 0.7 mV, n = 10. **(B)** Exemplar patch clamp records of WT KCNQ2 channels expressed in HEK293 cells. In control solution, cells were held at −120 mV, with depolarizations to +20 mV. 10 µM ICA73 was applied extracellularly for ∼1 min while holding at −120 mV. Cells were then depolarized again to +20 mV (first pulse in ICA73), with repeated depolarizations every 6 s (subsequent pulses in ICA73). **(C)** Instantaneous current (marked by asterisks in B) in the first pulse and subsequent pulses as a percentage of the peak current, calculated from cells which had drug applied during holding potentials of −120, −80, and −60 mV (n = 4–7). Hollow symbols are data from individual cells, and filled symbols are mean ± SEM. **(D)** Exemplar patch clamp records of KCNQ2 channels expressed in HEK293 cells, incubated in 10 µM ICA73 for 1 min. Cells were held at −100 mV before being depolarized to +20 mV for 200 ms (first sweep) and then hyperpolarized to −120 mV for 10 s. The duration of the depolarizing pulse increased by 500 ms in each subsequent sweep. **(E)** Tail currents at −120 mV (from D) were normalized to better visualize kinetic differences.

cation of Kv7 channels as targets for diseases of hyperexcitability has led to the development of a variety of openers (Miceli et al., 2008, 2018; Xiong et al., 2008) including phenamates (diclofenac and meclofenamic acid derivatives; Peretz et al., 2010), zinc pyrithione, (Xiong et al., 2007), BMS-204352, and the acrylamide compound (S)-1 (Bentzen et al., 2006). Last, a class of substituted benzamides including ICA-069673, ICA-27234, ICA-110381, ztz-240, and ML-213 exhibit activity as Kv7 openers (Wickenden et al., 2008; Gao et al., 2010; Yu et al., 2011). Of these, the most well documented in preclinical anticonvulsant models is ICA-27243, although our group has primarily used ICA-069673 (ICA73) to investigate the mechanism of action on KCNQ channels (Padilla et al., 2009; Wang et al., 2017).

Recognition of diverse mechanisms of action of KCNQ openers originated with the demonstration that ICA-27243 retained activity on mutant channels lacking the conserved pore Trp residue known to be essential for retigabine activity (Xiong et al., 2008; Padilla et al., 2009; Gao et al., 2010; Peretz et al., 2010). Moreover, ICA-27243 exhibited greater subtype specificity, enhancing Q2/3 current but not Q3/5 or Q3 homomeric current (Wickenden et al., 2008; Blom et al., 2010). A series of chimeric channels between drug-sensitive and insensitive subunits revealed that residues in the KCNQ2 voltage-sensing domain (VSD) were important for ICA73 and ICA-27243 effects, and our group recently identified two residues in the S3 helix of the KCNQ2 VSD that are critical for ICA sensitivity: A181 and F168 (Padilla et al., 2009; Wang et al., 2017). Mutations at either of these positions weaken or abolish ICA73-mediated gating effects but retain retigabine sensitivity. This provides further support that ICA73 and retigabine have distinct binding sites and may act through different mechanisms.

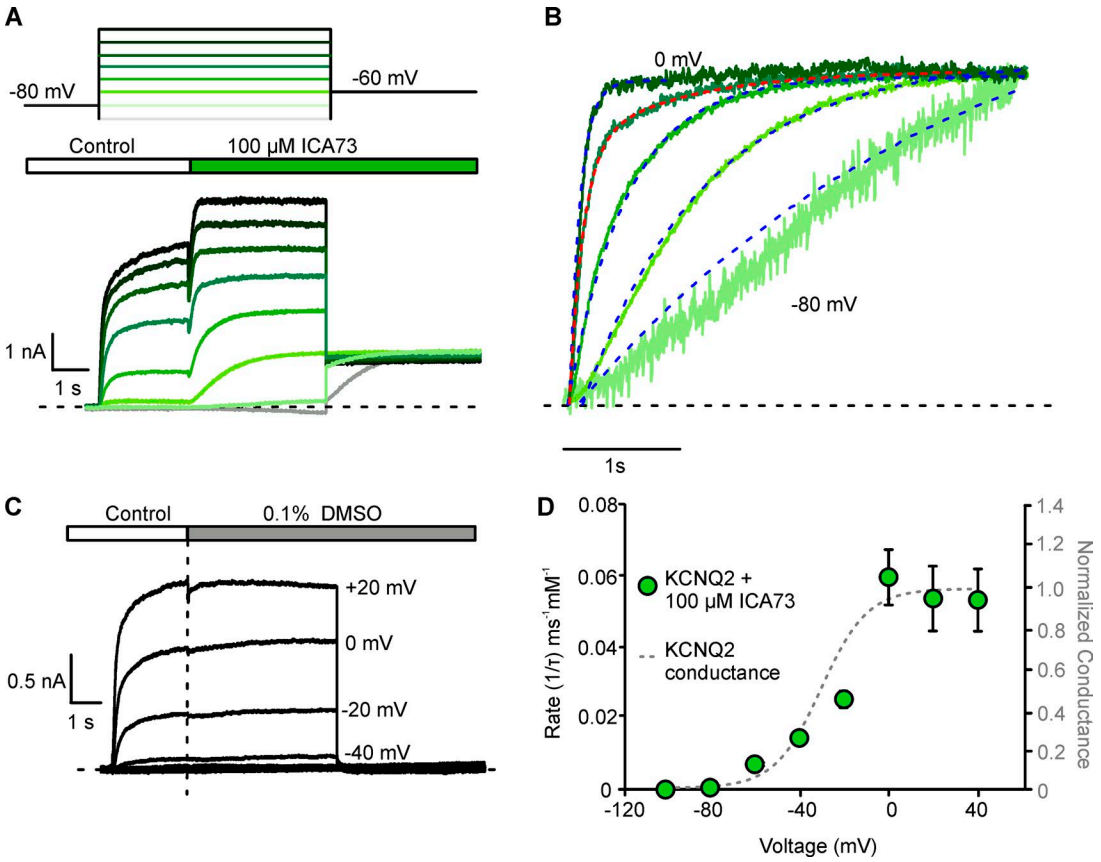

Figure 2. **The ICA73 binding kinetics correlate with KCNQ2 channel activation. (A)** Voltage protocol and exemplar current traces for KCNQ2 channels in HEK293 cells. Cells were held at −80 mV and pulsed to a range of voltages between −120 and 40 mV for 5 s. After 1 s at the test voltage, 100 µM ICA73 was applied rapidly. **(B)** Magnified view of the current traces immediately following ICA73 application, normalized to the peak current at −20 mV. Single exponential fits are superimposed in blue. Occasionally, a sum of two exponential equations was required (red fit), in which case the dominant component was used as a measure of interaction rate. Fits also excluded the first 30 ms after the solution exchange, which is contaminated by rapid block by DMSO. **(C)** Exemplar traces for WT KCNQ2 channels in HEK293 cells, with DMSO rapidly applied. Cells were held at −100 mV, then pulsed to a range of voltages between 0 mV and −100 mV for 2.5 s before DMSO application. Cells were then pulsed to −60 mV for 5 s. **(D)** Rates of ICA73 binding (green circles, left axis; *n* = 4–6) and KCNQ2 conductance-–voltage relationship in HEK293 cells (dotted line, right axis). Error bars represent mean ± SEM.

Use-dependent interactions are often considered to be a useful property of small-molecule ion channel modulators. The most widely studied example is use-dependent actions of many voltage-dependent sodium channel blockers, which preferentially stabilize the inactivated channel state and thereby exert stronger effects in hyperexcitable cells (Ragsdale et al., 1994). Although the anticonvulsant properties of KCNQ openers are well known, their use-dependent properties and fundamental mechanisms of action have not been described in detail. In this study, we characterized the state dependence of interaction of retigabine and ICA73 with homomeric KCNQ2 channels. Our findings demonstrate that in addition to acting via different binding sites, these compounds also have fundamentally different mechanisms of action. The ICA73 appears to bind almost exclusively to activated channel states. In contrast, retigabine exhibits less prominent state-dependent accessibility. Collectively with the differences in mutations that alter sensitivity to these drugs, our findings demonstrate the presence of at least two distinct mechanisms of action of KCNQ channel openers. We also characterize the effects of a voltage sensor mutation that alters sensitivity to ICA73.

Materials and methods

Electrophysiology

Patch pipettes were manufactured from soda lime capillary glass (Fisher), using a Sutter P-97 puller (Sutter Instrument). When filled with standard recording solutions, pipettes had a tip resistance of 1–3 MΩ. Recordings were filtered at 5 kHz; sampled at 10 kHz, with manual capacitance compensation and series resistance compensation between 70 and 90%; and stored directly on a computer hard drive using an Axopatch 200B amplifier, Digidata 1440 digitizer, and Clampex 10.7 software (Molecular Devices). Series access resistances did not exceed 5 MΩ (usually <3 MΩ). The KCNQ2 channels do not generate large currents in our experimental system (rarely >3 nA at 0 mV). The largest calculated voltage error (see +40 mV trace in Fig. 2 A) was ∼4 mV after 80% series resistance compensation (6 nA * 3 MΩ * [1–0.8]) = 3.6 mV. Bath solution had the following composition: 135 mM NaCl, 5 mM KCl, 1 mM $CaCl_2$, 1 mM $MgCl_2$, and 10 mM HEPES and was adjusted to pH 7.4 with NaOH. Pipette solution had the following composition: 135 mM KCl, 5 mM K-EGTA, and 10 mM HEPES and was adjusted to pH 7.2 using KOH. The pipette and bath solutions generate a calculated liquid junction potential of ∼4.3 mV that

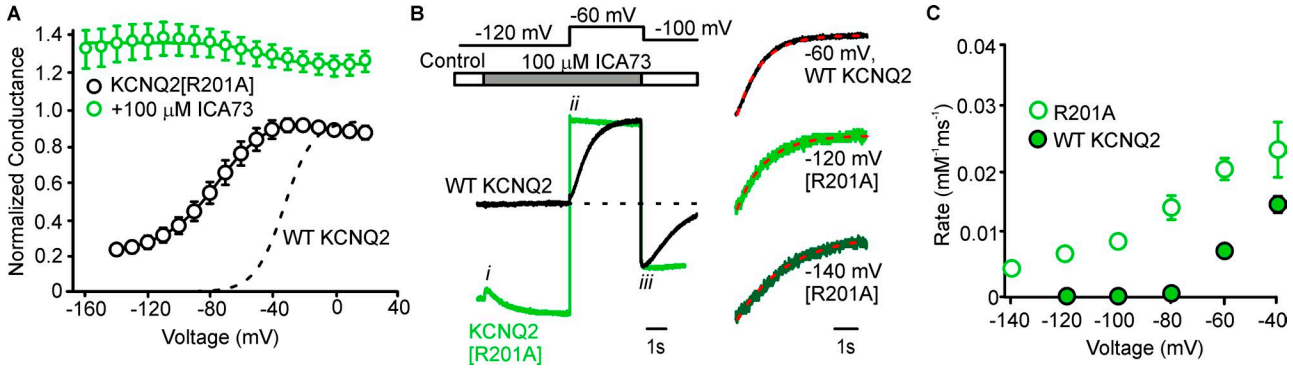

Figure 3. **The ICA73 accessibility shifts to negative voltages in a shifted KCNQ2 channel mutant. (A)** Conductance–voltage relationships for KCNQ2 [R201A] channels expressed in HEK293 cells in control (black circles) or 100 μM ICA73 (green circles). The voltage dependence of WT KCNQ2 channel opening in control is indicated by the dashed line. **(B)** Exemplar traces for WT KCNQ2 (black) and R201A (green) after rapid application of 100 μM ICA73 at −120 mV. The rates of ICA73-mediated current potentiation at −60 (WT), −120, and −140 mV (R201A) are also shown for comparison. **(C)** Rates of ICA73 binding to WT KCNQ2 (filled circles; n = 4–6) and R201A (unfilled circles; n = 3–6) are plotted against membrane voltage. Error bars in A and C represent mean ± SEM.

was not corrected for in the reported experiments. Chemicals were purchased from Sigma-Aldrich or Fisher. Solutions were delivered at room temperature (19–21°C) by pressure-driven flow, through a multibarreled solution delivery turret, driven by the RSC-200 (Biological) rapid solution exchanger to enable solution jumps.

Drug solutions

Retigabine was obtained from Toronto Research Chemicals, and ICA73 was obtained from Tocris. Drugs were dissolved in DMSO to yield stock concentrations of 100 mM. Stock solutions were diluted in extracellular solutions to appropriate concentrations for experiments the same day.

Ion channel constructs and expression in cell lines

Human KCNQ2 DNA originally expressed in pTLN vectors, obtained from Dr. M. Taglialatela (University of Naples, Italy) and Dr. T. Jentsch (Max-Delbrück-Centrum für Molekulare Medizin, Germany), were subcloned into pcDNA3.1 (-). The point mutant KCNQ2[A181P] was generated using a two-step overlapping PCR method, then subcloned into pcDNA3.1 using NheI and EcoRI restriction enzymes. Sequences were verified by Sanger sequencing approaches (Genewiz).

The HEK293 cells were maintained in Dulbecco's modified eagle medium supplemented with 10% FBS and 1% penicillin/streptomycin. Cells were grown in Falcon tissue culture–treated flasks, in an incubator at 5% CO_2 and 37°C. Cells were plated onto 12-well plates and allowed to settle for 24–48 h before transfection. Cells were transiently transfected with 1 μg of DNA encoding the channel of interest and 500 ng of GFP, using jetPRIME DNA transfection reagent (Polyplus). 24 h after transfection, cells were plated onto sterile coverslips for electrophysiology experiments the following day. Transfected cells were selected/excluded from recordings based on GFP fluorescence and current magnitude. No cells used for data analysis had currents <500 pA at −20 mV. There is also an endogenous K^+ current present in the HEK cells used for our recordings. However, the endogenous current is clearly distinguishable from KCNQ2 currents because it has notably faster activation kinetics and does not activate until depolarized voltages near +20 mV. An example of some minor contamination can be as a small (~200-pA) rapid activation component (see Fig. 4 D).

Data analysis

Conductance–voltage relationships were normalized to the peak conductance in control conditions and fit with a Boltzmann equation:

$$\frac{I}{Imax} = \frac{A}{1 + e^{-(V-V_{1/2})/k}},$$

where A is the ratio of the peak conductance (normalized to peak conductance in control conditions), $I/Imax$ is the normalized tail current magnitude, V is the voltage applied, $V_{1/2}$ is the half activation voltage, and k is a slope factor reflecting the steepness of the curve. Conductance–voltage relationships from individual cells were fit using a least-squares minimization approach in Microsoft Excel (Solver tool), followed by calculation of descriptive statistics for individual fit parameters (mean ± SEM are used throughout the text). Kinetics of current relaxation were fit with a single exponential time course using Clampfit. Occasionally, the sum of two exponentials was required to achieve a good fit because of the presence of a slow activation component. In that case, the dominant time constant was used for calculation of the rate of drug interaction.

Results

The ICA73 binding is occluded in the KCNQ2 closed state

Application of ICA73 to homomeric KCNQ2 channels causes a dramatic hyperpolarizing gating shift, ~50% current potentiation at voltages where the activation curve is saturated, and deceleration of channel deactivation (Fig. 1 A; Wang et al., 2017). We investigated state-dependent interaction of ICA73 and KCNQ2 by applying 10 μM ICA73 for ~1 min while holding the membrane potential at various negative voltages (Fig. 1, B and C). We assessed drug interactions with the channel during the wash-in and incubation,

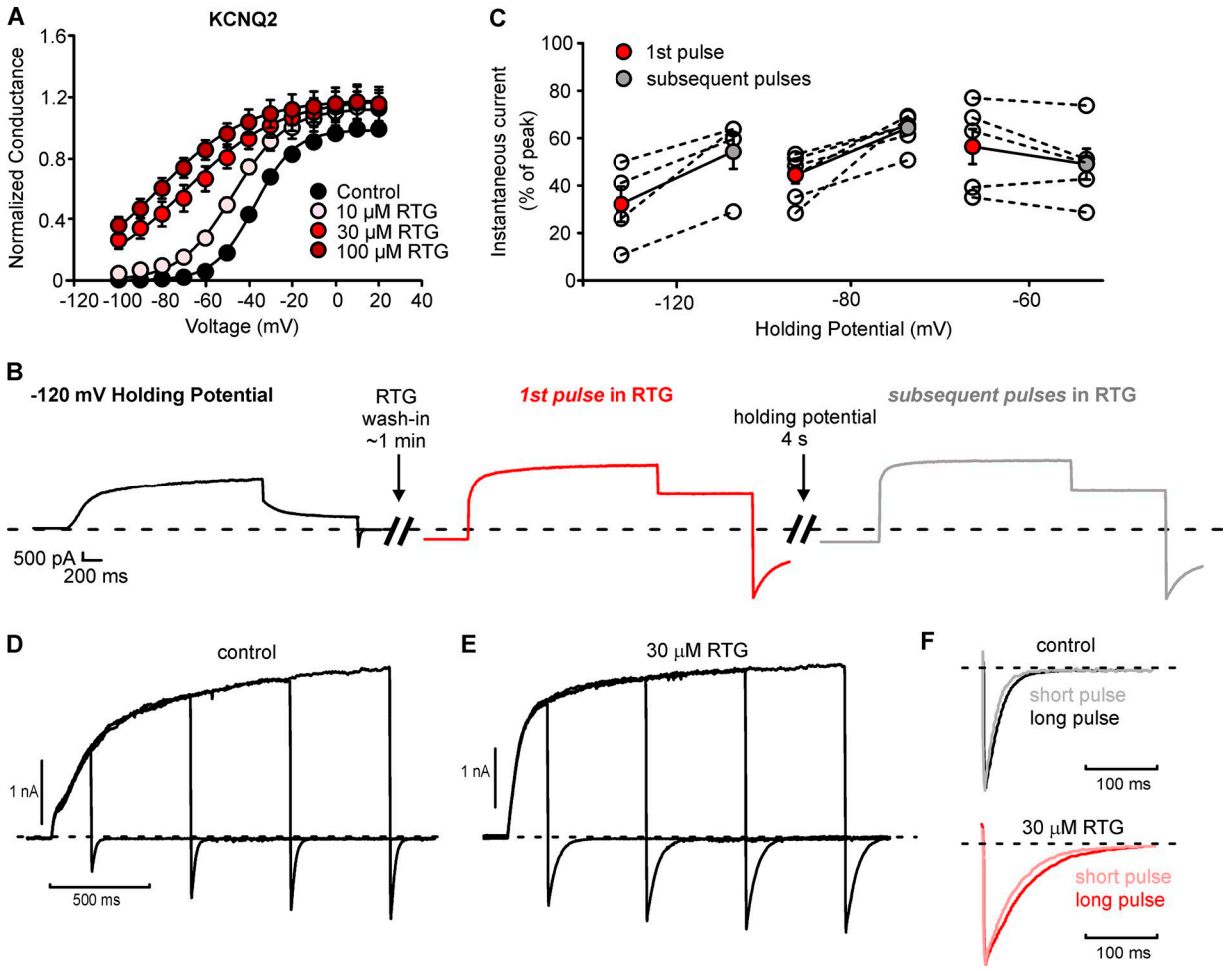

Figure 4. **Retigabine can access open and closed channels. (A)** Conductance–voltage relationships for WT KCNQ2 channels expressed in *X. laevis* oocytes in various concentrations of retigabine (RTG), normalized to peak current in control for each cell. The KCNQ2 parameters of activation were as follows: control $V_{1/2}$ = −36.8 ± 1.1 mV, k = 9.2 ± 0.4 mV; 10 µM RTG $V_{1/2}$ = −47.6 ± 2.0 mV, k = 12.2 ± 1.1 mV; 30 µM RTG $V_{1/2}$ = −69.5 ± 5.4 mV, k = 21.6 ± 2.0 mV; and 100 µM RTG $V_{1/2}$ = −81.7 ± 3.6 mV, k = 20.7 ± 1.4 mV, n = 6. Error bars represents mean ± SEM. **(B)** Wash-in experiment described in Fig. 1 B was performed using 30 µM RTG. Records depict the experiment with a holding potential of −120 mV. **(C)** Instantaneous current as a percentage of peak current, calculated from cells which had drug applied at holding potentials of −120, −80, and −60 mV (n = 4–6). Hollow symbols are data from individual cells, and filled symbols represent the mean ± SEM. **(D and E)** Exemplar patch clamp records of WT KCNQ2 channels expressed in HEK293 cells, in control (D) or after incubation in 30 µM RTG for 1 min (E). Cells were held at a holding potential of −100 mV before being depolarized to +20 mV for 200 ms (first sweep), then hyperpolarized to −120 mV for 5 s. The duration of the depolarizing pulse increased by 500 ms in each subsequent sweep. **(F)** Current traces from D and E were normalized to better visualize kinetic differences.

based on the development of a standing current. When cells are held at −120 mV, incubation in 10 µM ICA73 fails to generate any apparent standing current (or instantaneous current upon depolarization) until after the first depolarizing pulse following drug application (Fig. 1 B). However, upon the first depolarization in the presence of ICA73, there is development of a potentiated outward current with nearly identical kinetics to the control pulse (Fig. 1 B, inset normalized activation) and a dramatically decelerated tail current (Fig. 1 B, green) that prevents channel closure before a subsequent pulse 4 s later, leading to a large instantaneous current in subsequent pulses (Fig. 1 B, gray). Application of ICA73 at more depolarized holding voltages caused development of a more prominent standing current during the drug incubation period (Fig. 1 C). These findings indicate that ICA73 interactions with KCNQ2 are influenced by the holding potential, and access to the channel becomes very slow at negative voltages.

This occlusion of ICA73 from resting states is also apparent in the development of the ICA73-mediated slow tail currents (Fig. 1 D). In this experiment, cells were depolarized to +20 mV for varying durations in 10 µM ICA73. The short depolarization (200 ms) elicits primarily rapid deactivation kinetics, whereas a slow component of deactivation becomes much more prominent as the duration of the depolarizing pulse is prolonged (exemplar tails for 200 ms vs. 1,700 ms depolarizations are presented in Fig. 1 E).

The ICA73 binding site access tracks voltage-dependent activation

The ICA73 interactions with the channel were investigated with greater time resolution using rapid solution exchange over a range of voltages (Fig. 2). Cells were stepped between −100 and 40 mV for 1 s, followed by rapid application of 100 µM ICA73

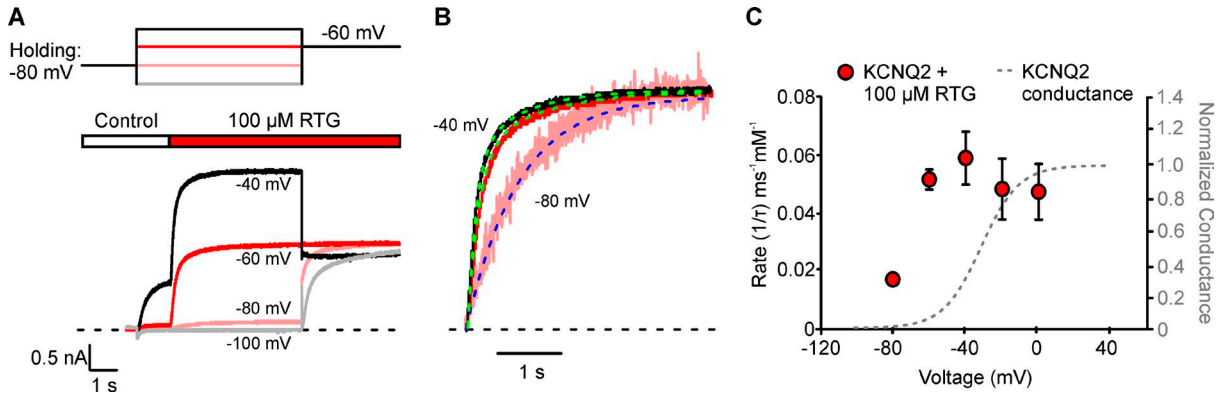

Figure 5. **Retigabine interacts with resting channels. (A)** The voltage and timed perfusion protocol described in Fig. 2 A was performed using 100 µM RTG. Exemplar current traces from cells expressing WT KCNQ2 channels are shown. **(B)** Magnified view of the current traces immediately following RTG addition, normalized to peak current. Single exponential fits are superimposed in blue. Occasionally, a sum of two exponential equations was required (green fits), in which case the dominant component was used as a measure of interaction rate. Fits also excluded the first 30 ms after the solution exchange, which is contaminated by rapid block by DMSO as described in Fig. 2 C. **(C)** Rates of RTG binding (red circles, left axis; *n* = 2–7) and KCNQ2 conductance–voltage relationship in HEK293 cells (dotted line, right axis). Error bars represent mean ± SEM.

(Fig. 2 A). Based on calibrations with K^+ concentration jumps, we estimate that the time constant of solution exchange in these experiments is ∼20 ms (Zhang et al., 2015). The rate of ICA73 interaction with KCNQ2 channels was estimated using the rate of current increase upon drug application. These effects are dependent on ICA73, as identical experiments performed with an equivalent of DMSO (used to generate ICA73 stock solutions) exhibit no current potentiation. The DMSO application causes a very minor rapid blockade (Fig. 2 C) and can also be observed as a small negative current deflection immediately upon drug delivery in Fig. 2 A. In the absence of clear channel opening (at very negative voltages), we could also roughly infer the extent of drug binding based on the properties of current activation in a subsequent pulse to −60 mV (Fig. 2 A).

In the absence of ICA73, only a small fraction of KCNQ2 channels are activated at −60 mV. Upon rapid application of 100 µM ICA73, there is a slow but resolvable current increase (Fig. 2 A). At more positive voltages, the rate of ICA73 current enhancement is accelerated, as exemplified in normalized traces (Fig. 2 B). In contrast, at −100 mV or more negative voltages, ICA73 interactions are very slow because the subsequent pulse to −60 mV exhibits little or no instantaneous current (Fig. 2 A). Also, the time course of activation at −60 mV (after a −100-mV prepulse) is similar to activation after rapid drug application at −60 mV (Fig. 2 A). This observation implies that drug application at −100 mV (or more negative voltages) has a minimal effect until the step to −60 mV, at which point channels behave as if they were rapidly exposed to the drug.

We quantified the rate of interaction as a function of membrane voltage at the time of drug application (Fig. 2, B and D) and plotted these data together with the conductance–voltage relationship, highlighting that the rate of ICA73 interaction closely tracks the voltage dependence of channel activation. Sample single-exponential fits are shown as dashed blue lines (Fig. 2 B), and for clarity, we should mention that occasionally there is a slow activation component that requires a sum of two exponentials to fit (red fit in Fig. 2 B). In those cases, the dominant time constant describing the most significant fraction of current activation was used to assess the rate of drug interaction. Also, at negative voltage the rate becomes difficult to assess precisely because they are slow and begin to appear more sigmoidal. At −80 mV (Fig. 2 B), we further constrained the fit based on the observation that maximal activation is achieved in 100 µM ICA73 at −80 mV (Fig. 1 A).

In these experiments, the rate of interaction varies substantially (∼150-fold) with voltage, from 0.00038 ± 0.00007 ms^{-1} mM^{-1} at −80 mV to 0.060 ± 0.008 ms^{-1} mM^{-1} at 0 mV. At more negative voltages, we could estimate an upper bound for the rate of interaction based on the magnitude of instantaneous current observed in the step to −60 mV. At −100 mV, there is occasionally a small but convincing instantaneous current (Fig. 2 A), but this is no larger than 20% of the instantaneous current generated by the −80 mV pulse (suggesting ∼750-fold slower access of ICA73 relative to the saturating rate at 0 mV). At more negative voltages, rates are so slow that we cannot confidently measure them in this experiment. The implication of this observation is that the degree of channel activation limits the rate of ICA73 access to its binding site. An important related finding is that the conductance–voltage relationship of KCNQ channels has been previously shown to closely overlap with the voltage dependence of voltage sensor movement (Osteen et al., 2012; Kim et al., 2017). Thus, we suggest that voltage sensor movement gates access to a binding site for ICA73.

We explored these observations further by measuring rates of ICA73 interaction with the KCNQ2[R201A] mutant. This mutation is equivalent to the previously reported KCNQ1[R231C] channel and exhibits a gain of function phenotype arising from a hyperpolarizing shift of the voltage dependence of activation (Fig. 3 A; Osteen et al., 2012). Using similar voltage and solution exchange timing as in Fig. 2, we observed that KCNQ2[R201A] channels exhibited current potentiation leading to complete channel activation at very negative voltages (−120 and −140 mV are shown in Fig. 3 B). In the exemplar data, we have highlighted three regions of interest for direct comparison to WT KCNQ2. In region i, 100 µM ICA73 is rapidly applied, leading to current potentiation of KCNQ2[R201A] but no effect on WT KCNQ2. In region ii (step to −60 mV), it is apparent that ICA73 exposure at

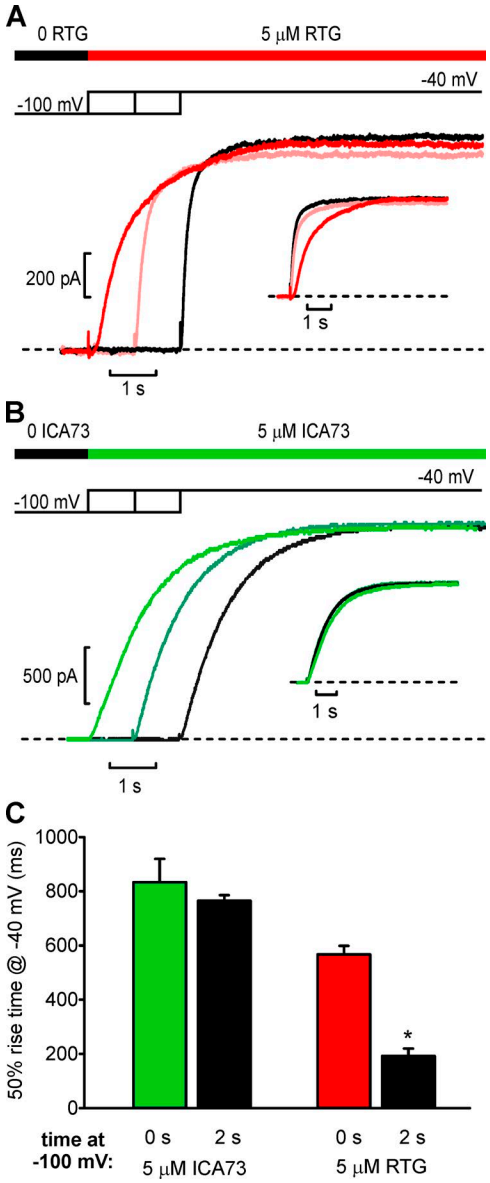

Figure 6. **Acceleration of KCNQ2 activation after retigabine exposure at negative voltages. (A)** 5 μM retigabine was applied to HEK 293 cells expressing WT KCNQ2 channels, for varying durations (0, 1, or 2 s) at −100 mV, followed by a voltage step to −40 mV. **(B)** Identical solution and voltage steps were applied as in A but with 5 μM ICA73. **(C)** Summary data illustrating the 50% rise time of current upon depolarization to −40 mV for ICA73 (n = 3) or retigabine (n = 5), illustrating retigabine-mediated acceleration of channel activation after a 2-s exposure at −100 mV (Student's t test compared the 0- and 2-s exposures in each drug; *, $P < 0.05$ relative to the 0-s exposure). Error bars represent mean ± SEM.

−120 mV leads to complete activation of KCNQ2[R201A] but has no effect on WT KCNQ2 until the voltage is stepped to −60 mV. Last, in region iii, it is apparent that closure of [R201A] channels is extremely slow in these conditions, likely because of the intrinsic bias of these channels toward the activated state. Across a range of negative voltages, KCNQ2[R201A] exhibits potentiation by ICA73, whereas WT KCNQ2 is not responsive (Fig. 3 C). This finding demonstrates that accessibility of ICA73 depends on channel conformation, and accessibility at more negative voltages is only apparent in mutants with shifted voltage-dependent gating.

Retigabine readily accesses KCNQ2 closed states

As mentioned, previous reports have suggested a distinct binding site for ICA73 (in the voltage sensor) versus retigabine (in the pore; Padilla et al., 2009; Wang et al., 2017). To compare the mechanism of action of retigabine and ICA73, we performed similar wash-in experiments with 30 μM retigabine, revealing significant differences in channel responses at hyperpolarizing voltages. The effects of retigabine on the KCNQ2 conductance–voltage relationship and deactivation kinetics are much less pronounced than ICA73 (Fig. 4 A). However, incubation in 30 μM retigabine caused development of a prominent standing current over a wide voltage range (−120 to −60 mV), and acceleration of channel activation is apparent in the presence of retigabine, as previously reported (Main et al., 2000; Wickenden et al., 2000). In contrast to ICA73 (Fig. 1), these findings indicate that retigabine can more readily access resting states of the channel. It was also clear that both short and long depolarizations in retigabine generated deceleration of tail current kinetics (Fig. 4, D–F). This finding contrasts with the effects of ICA73 using similar experimental protocols (Fig. 1, D and E) and suggests that retigabine interacts readily with channel resting states.

Using rapid solution exchange for time-resolved retigabine application, we confirmed that drug association is rapid even at voltages where channels are predominantly closed (Fig. 5). As noted previously, some traces required a sum of two exponentials (highlighted in green in this cases), and we used the dominant time constant to assess the interaction rate. At −80 mV, although currents are small (close to the reversal potential for potassium), the onset of channel opening after retigabine application can still be resolved and is only modestly slower (0.018 ± 0.001 $ms^{-1}\,mM^{-1}$) than at 0 mV (0.05 ± 0.01 $ms^{-1}\,mM^{-1}$; Fig. 5, B and C). This finding suggests retigabine interaction with KCNQ2 channels is not gated by channel opening and closing. However, there does appear to be a steep voltage-dependent change in the rate of retigabine-mediated current potentiation between −60 and −80 mV (Fig. 5, B and C). Unlike ICA73 (Fig. 3), this reduction in rate does not coincide with the voltage dependence of channel activation. Also, voltage clamp fluorometry and gating current records from other KCNQ channel types (KCNQ1, KCNQ3, and KCNQ4) indicate that voltage sensor movement has similar voltage dependence to channel activation (Miceli et al., 2009; Osteen et al., 2012; Kim et al., 2017). Although we cannot correlate this change in rate with an experimentally observable state transition, another possibility is that retigabine is occluded from a state early in the activation pathway.

We further investigated retigabine interactions with KCNQ2 channels at negative voltages, keeping in mind other observations related to retigabine association with preopen states. Most importantly, channel activation is consistently accelerated in the presence of retigabine (Fig. 4, D and E, and also further characterization in Fig. 6). This differs from ICA73 (Fig. 1 B) and implies that retigabine can bind to resting channel states (or binds to some preopen state in the activation pathway and accelerates subsequent steps). We performed additional rapid perfusion ex-

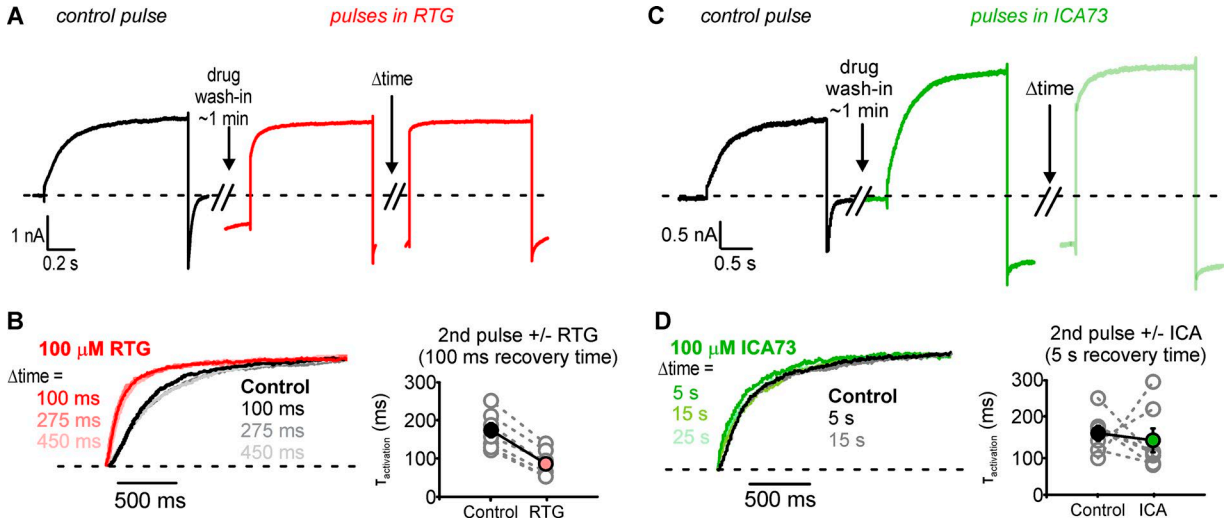

Figure 7. **Differential effects of RTG and ICA73 on KCNQ2 activation kinetics. (A and C)** Exemplar patch clamp records of WT KCNQ2 channels before and after exposure to RTG or ICA73. Under control conditions, cells were held at −100 mV, depolarized to 0 mV, and repolarized to −100 mV while drug was applied (1-min wash-in). Cells were then depolarized to 0 mV (2 s) and returned to −100 mV for varying durations (Δtime) to allow partial channel closure. **(B and D)** Exemplar current traces showing kinetics of the activating fraction of current in RTG or ICA73 (red and green, respectively, after varying durations of repolarization) or control solution (black), normalized to the peak current after drug. Activation time constants in control or drug conditions (n = 7) are depicted on the right. Hollow symbols are data from individual cells, and filled symbols are mean ± SEM.

periments using lower ICA73 and retigabine concentrations to distinguish the apparent drug interaction rate from channel gating. We measured channel behavior when 5 µM retigabine was applied simultaneously with a voltage step to −40 mV and compared this with channel activation observed after brief (1–2 s) retigabine applications at −100 mV (Fig. 6 A). The rate of current increase is slow when retigabine is applied simultaneously with a step to −40 mV, reflecting a combination of channel activation and slow drug association. In contrast, if 5 µM retigabine is applied while channels are held at −100 mV for 1 or 2 s, subsequent steps to −40 mV exhibit much faster activation. This finding suggests that channels have bound the drug while at −100 mV, enabling rapid activation upon depolarization to −40 mV. This behavior contrasts with ICA73 in identical experiments (Fig. 6 B). When 5 µM ICA73 is applied simultaneously with a voltage step to −40 mV, there is a slow rate of current increase. Unlike for retigabine, kinetics of channel activation at −40 mV are not altered if ICA73 is preapplied at −100 mV, consistent with our prior conclusion that ICA73 is strongly excluded when channels are held at −100 mV. Although the effects of these drugs are qualitatively consistent, there is often variation in the appearance of multiple activation components between cells. Therefore, we compared the effects of ICA73 and retigabine by measuring the 50% current rise time (Fig. 6 C), highlighting the retigabine-mediated acceleration of channel activation observed when the drug is administered at −100 mV.

From observations like these, we infer that significant association of retigabine occurs even during brief exposures at negative voltages because channel activation is accelerated in subsequent depolarizing steps. Revisiting the apparent volt-

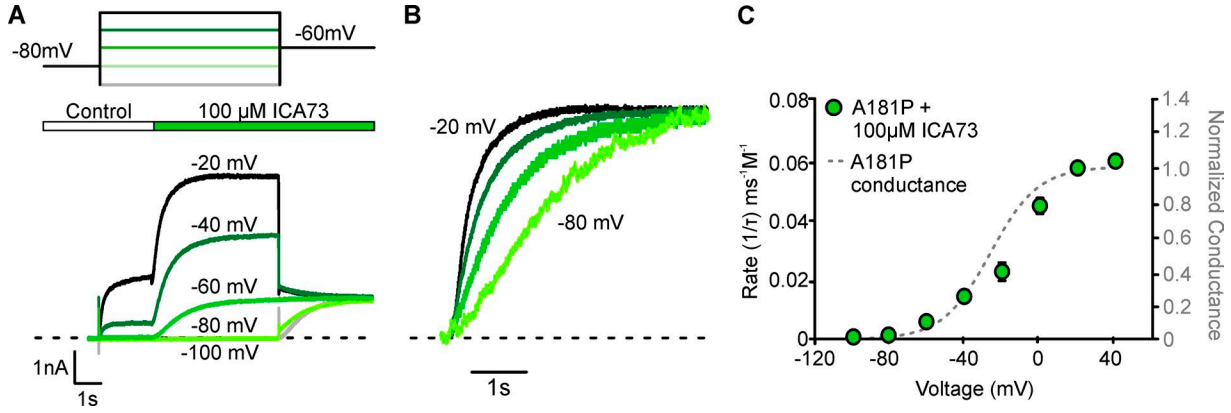

Figure 8. **The ICA73 binding to KCNQ2[A181P] correlates with channel activation. (A)** The voltage and timed perfusion protocol described in Fig. 2 A was performed using 100 µM ICA73 with KCNQ2[A181P] channels. Exemplar current traces from cells expressing KCNQ2[A181P] channels are shown. **(B)** Magnified view of current traces immediately following drug addition, normalized to highlight interaction kinetics with ICA73. **(C)** Rates of ICA73 binding (green circles, left axis; n = 2–6) and KCNQ2[A181P] conductance–voltage relationship in HEK293 cells (dotted line, right axis). Error bars represent mean ± SEM.

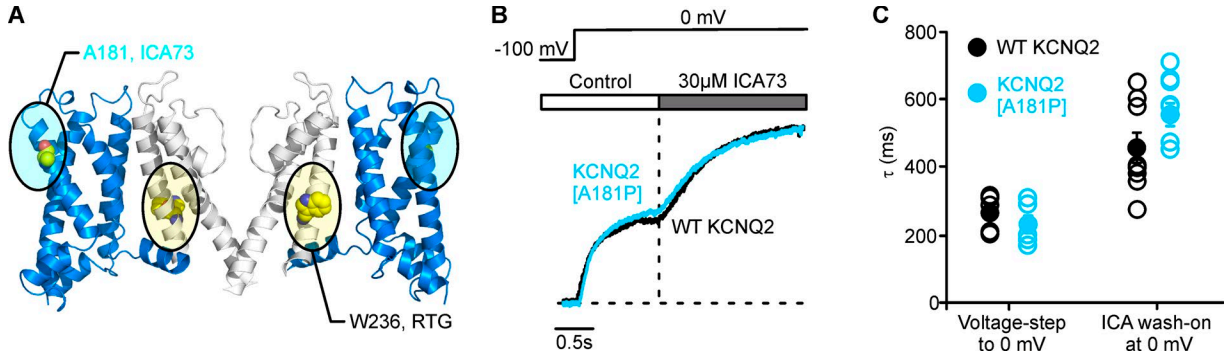

Figure 9. **The ICA73 binding is not affected in KCNQ2[A181P] channels. (A)** Model of KCNQ2 channel structure, highlighting the location of A181 in the voltage-sensing domain (highlighted in blue), distant from W236 that forms the canonical RTG binding site in the pore domain (yellow). **(B)** Exemplar current traces for WT KCNQ2 channels (black) and KCNQ2[A181P] channels (blue). Cells were held at −100 mV and depolarized to 0 mV, during which time 30 μM ICA73 was rapidly applied extracellularly. **(C)** Activation time constants of channel opening by a voltage step to 0 mV and following rapid drug application at 0 mV (n = 5–6). Hollow symbols are data from individual cells, and filled symbols are mean ± SEM.

age-dependent reduction in the rate of retigabine interaction in Fig. 5 C, we should mention the shortcoming of using currents as a proxy for measuring drug binding. In the case of retigabine, this is a challenge at more negative voltages (e.g., −80 and −100 mV) because a significant fraction of channels remain closed, even in saturating retigabine concentrations (Fig. 4 A). Thus, the rate that is attributed to retigabine association (e.g., Fig. 5 B; −80 mV) is likely strongly influenced by the gating transitions of retigabine-bound channels at these negative voltages (and high retigabine concentrations). Note that the effects of 5 μM retigabine appear complete after ∼2 s at −100 mV (Fig. 6 A), comparable to the rate of current enhancement in 100 μM retigabine despite a 20-fold lower concentration (Fig. 5 B). This observation suggests that retigabine association in saturating conditions occurs faster than we can detect based on current measurements in Fig. 5 B and that the measured rate reflects gating transitions of channels that are already bound to retigabine. This is also consistent with the observation that voltage-dependent changes in retigabine rates (Fig. 5 C) occur in approximately the same voltage range as the fully shifted conductance–voltage relationship of KCNQ2 in saturating retigabine concentrations ($V_{1/2}$, approximately −80 mV; Fig. 4 A).

Channel closure requires ICA73 unbinding

Findings thus far suggest marked differences in the state accessibility of ICA73 and retigabine. We further investigated the state accessibility of these KCNQ openers by examining channel reopening in the presence of retigabine and ICA73. We had noted that activation kinetics of KCNQ2 in the presence of ICA73 were not altered significantly from control conditions, in contrast to the pronounced acceleration of channel activation observed in the presence of retigabine (Figs. 1, 2, 3, 4, 5, and 6). We reasoned that this is likely a reflection of different closed state binding properties of these drugs. That is, accelerated activation kinetics in the presence of retigabine might indicate binding and destabilization of resting states. In contrast, closed KCNQ2 channels appear to have much lower accessibility for ICA73 and therefore would be predicted to activate with kinetics similar to control (and subsequently bind the drug after they reach an activated state). To test this difference, we delivered a depolarizing stimulus (0 mV) in the presence of each drug, repolarized for varying durations (Δ time in Fig. 7, A and C), to allow varying degrees of channel closure, and then depolarized again. We compared the activation kinetics of channels that closed during the repolarizing interpulse interval with activation kinetics in control conditions (normalized traces in Fig. 7, B and D; multiple repolarization times are highlighted in different shades). In retigabine, the activating fraction consistently exhibited accelerated activation kinetics (Fig. 6 B and inset), suggesting that retigabine remains associated with channels during repolarization-induced closure, leading to accelerated activation during subsequent depolarizations.

The ICA73 has much more prominent effects on channel deactivation, requiring up to 20-s repolarizations for complete channel closure at −120 mV (Fig. 7 C). Using longer interpulse intervals to achieve intermediate levels of channel closure, we observed that activation kinetics were unchanged relative to the control condition. We interpret this result to mean that channel closure requires ICA73 unbinding. Thus, channels that close during the interpulse interval are no longer bound to ICA73 and therefore exhibit activation kinetics identical to control conditions (Fig. 7 D).

A voltage sensor mutation accelerates ICA73 unbinding

We recently described the KCNQ2[A181P] mutation that attenuates ICA73-mediated gating effects but preserves current potentiation (Wang et al., 2017). Specifically, KCNQ2[A181P] mutant channels exhibit modest deceleration of channel deactivation in the presence of ICA73, leading to a weaker apparent shift of the conductance–voltage relationship relative to WT KCNQ2. The specific mechanism underlying this effect was not clear, and we speculated that this weaker gating effect might reflect a loss of the strict state dependence of ICA73 (allowing KCNQ2[A181P] channels to close even when bound to ICA73) or, alternatively, a faster unbinding rate reflecting weakened affinity.

We tested these possibilities using rapid solution application, as described in Figs. 2 and 5. This experiment demonstrates that ICA73 association with KCNQ2[A181P] becomes very slow at neg-

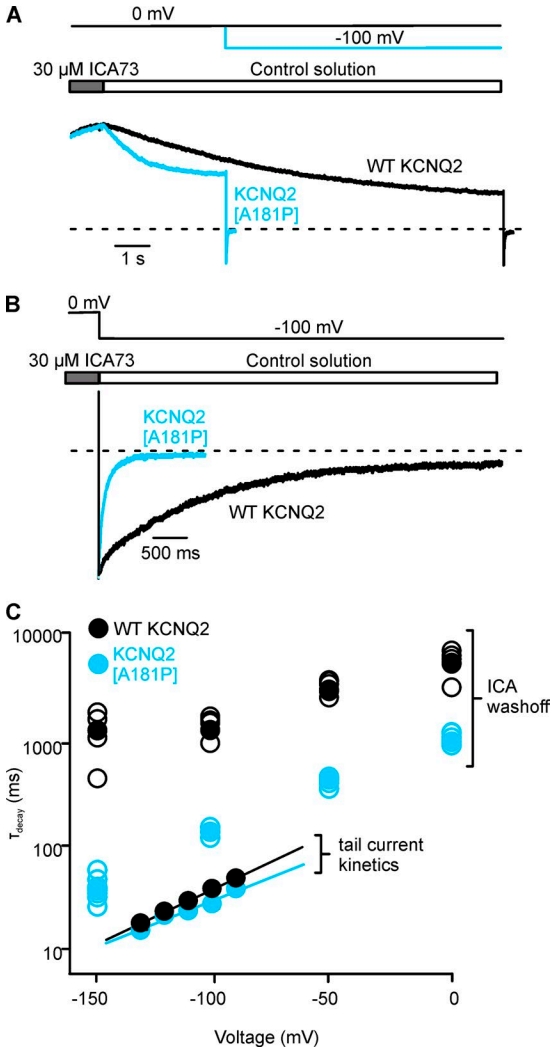

Figure 10. **Accelerated ICA73 unbinding from KCNQ2 [A181P] channels. (A and B)** Exemplar current recordings for WT KCNQ2 (black) and KCNQ2[A181P] (blue), following rapid washout of 30 µM ICA73 from bath at 0 (A) or −100 mV (B). **(C)** Time constants of current decay at 0, −50, −100, and −150 mV after rapid ICA73 washout (n = 4–6). Also depicted are deactivation tail current kinetics between −90 and −130 mV after a depolarizing prepulse to 0 mV (tail current kinetics; n = 5). Hollow symbols are data from individual cells, and filled symbols are mean ± SEM.

ative voltages, similar to what was observed for WT KCNQ2 (Figs. 2 and 7). There is a pronounced voltage dependence of ICA73 interaction with KCNQ2[A181P] channels, which tracks the voltage dependence of A181P conductance. The onset of ICA73 effects are extremely slow or absent at voltages more negative than −80 mV (Fig. 8, B and C).

We also compared the association and dissociation rates of ICA73 in WT KCNQ2 and KCNQ2[A181P] channels using rapid solution exchange (Figs. 9 and 10). Drug binding at 0 mV had similar time constants of ∼500 ms between WT KCNQ2 and KCNQ2[A181P] channels, suggesting that ICA73 binding is not strongly affected by the A181P mutation. This experiment differs slightly from Fig. 7 in that we focused on applying the drug at voltages where channels were fully activated and the ICA73 binding site was maximally accessible. Thus, channel transitions between resting and activated states would not influence the observed rate of interaction.

When ICA73 is rapidly washed off, there is very slow relaxation of currents in WT KCNQ2 channels, ranging from a time constant of ∼6 s (at 0 mV) to ∼2 s (at −150 mV; Fig. 10). This likely reflects very slow dissociation of ICA73 from the channels. Across all voltages tested, ICA73 dissociation from A181P channels was considerably faster (∼10-fold) than dissociation from WT KCNQ2, suggesting that the primary mechanism underlying the weakened ICA73 gating effects in KCNQ2[A181P] channels is accelerated unbinding reflecting weakened affinity, allowing for more rapid channel closure at negative voltages. Superimposed on these data in Fig. 10 C is the voltage dependence of channel closure for WT KCNQ2 and KCNQ2[A181P] channels. In the absence of ICA73, KCNQ2 and A181P channels deactivate with comparable kinetics, so intrinsic differences in channel gating do not account for the dramatic difference in ICA73 unbinding.

Discussion

Retigabine-sensitive KCNQ channel isoforms (KCNQ2-5) have been targeted in the development of voltage-gated potassium channel openers (Barrese et al., 2018; Miceli et al., 2018). Large compound libraries have been screened in recombinant systems and animal models, and several reports have documented openers with enhanced subtype specificity and increased potency toward certain KCNQ channel types (Padilla et al., 2009; Blom et al., 2010; Brueggemann et al., 2014). Some openers, such as ICA73, cause extremely large gating effects relative to retigabine on certain KCNQ subtypes, such as KCNQ2. Although many KCNQ channel openers act on the canonical retigabine site formed by a conserved Trp residue in the pore domain (Bentzen et al., 2006; Lange et al., 2009), it is now recognized that certain KCNQ openers are resistant to mutation of the retigabine site and instead act at an alternative voltage sensor site (Padilla et al., 2009; Gao et al., 2010; Peretz et al., 2010; Li et al., 2013; Wang et al., 2017). Consistent with this finding, point mutations in the voltage sensor (KCNQ2 A181 and F168) alter sensitivity to VSD-targeted drugs like ICA73 but not retigabine (Wang et al., 2017).

These structure–function approaches provide strong evidence for an alternative site for KCNQ openers, formed by the voltage sensor, in addition to the pore-delimited retigabine site. In this study, we used rapid solution switching to demonstrate fundamentally different mechanisms of action for pore- (retigabine) versus voltage sensor–targeted (ICA73) KCNQ openers. Most convincingly, the rate of ICA73 association with KCNQ2 closely tracks the voltage dependence of channel activation, whereas the rate of retigabine access is affected by membrane voltage much less prominently (Figs. 2 and 5). The ICA73 association with resting states of the channel is extremely slow (possibly completely occluded), as incubation of KCNQ2 in ICA73 has no effect on channel opening until a depolarization is delivered, channels open, and the binding site becomes accessible (Fig. 1). In contrast, retigabine association with KCNQ2 does not follow the same strict dependence on channel activation, and drug effects are apparent during retigabine incubation at negative voltages where most channels are closed. Hints of this dependence on

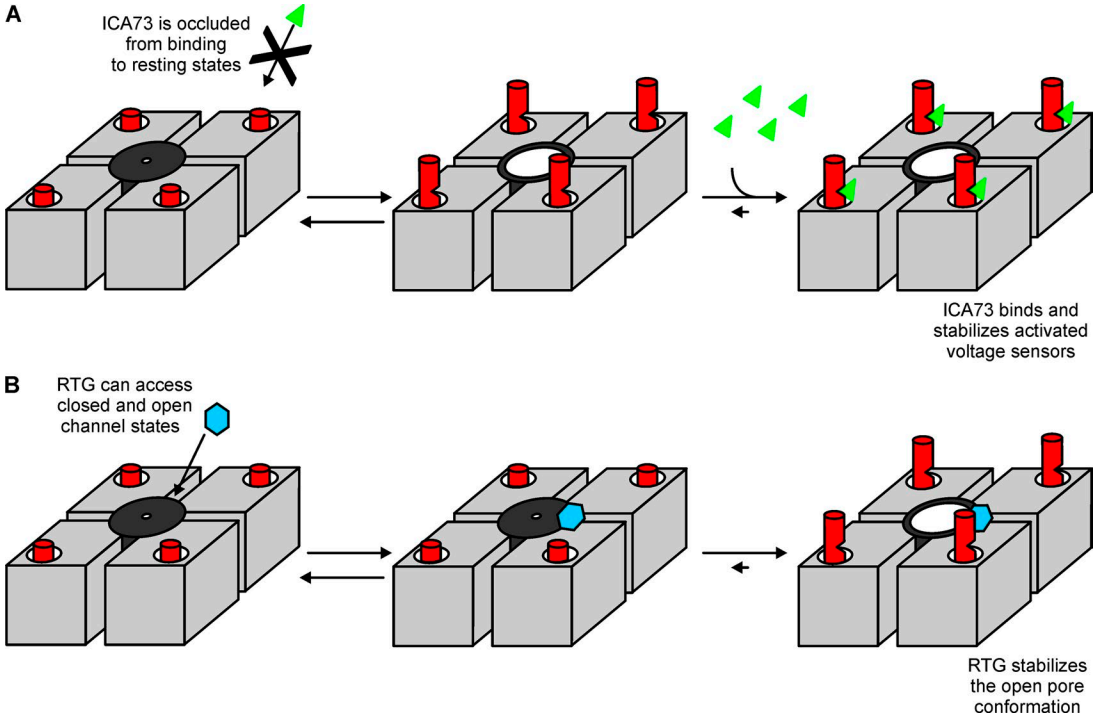

Figure 11. **Distinct binding sites and state dependence of RTG and ICA73. (A)** Schematic diagram of the mechanism of action of ICA73, targeting a binding site in the voltage-sensing domain. The ICA73 is proposed to interact nearly exclusively with the activated conformation of the voltage sensor, leading to stabilization of the activated state. **(B)** Schematic diagram of the mechanism of action of RTG, with a binding site in the pore domain. The RTG interacts with the pore domain in activated and resting conformations.

channel activation have appeared in pharmacological investigations of spinal reflexes, in which pore-targeted activators (retigabine, ML-213) rapidly suppress responses evoked by dorsal root stimulation, whereas ICA73 has a slower onset (many action potentials fire before the drug effect becomes apparent; Vicente-Baz et al., 2016).

Synthesizing data from mutagenesis and rapid solution perfusion, a reasonable explanation for our findings is that ICA73 (and likely related compounds like ICA-27243) binds nearly exclusively to activated states of the voltage-sensing domain. Thus, when channels are at rest, very few (if any) bind to ICA73, and activation kinetics are comparable to control conditions. After a voltage sensor reaches an active state, ICA73 can bind and dramatically decelerate voltage sensor deactivation, causing homomeric KCNQ2 channels to be trapped in an activated conformation for extended durations (Fig. 11 A). This pronounced state dependence differs significantly from retigabine (Fig. 11 B). The distinct mechanisms of action of these drugs are consistent with our recent findings that the stoichiometric requirement for channel activation is different for pore- versus VSD-targeted openers. The KCNQ3 activation by retigabine is nearly maximal in tetramers with a single retigabine-sensitive subunit. In contrast, ICA73 activation of KCNQ2 requires four drug-sensitive subunits for maximal drug effect, leading us to suggest that this multisubunit dependence may be caused by unique features of VSD–pore coupling in KCNQ channels (Wang et al., 2018; Yau et al., 2018). That is, activation of intermediate numbers of voltage sensors may underlie channel states with intermediate open probability or conductance.

Although the existence of an alternative VSD-delimited binding site is supported by several prior findings (Padilla et al., 2009; Gao et al., 2010; Peretz et al., 2010; Wang et al., 2017), details of the structural determinants of this binding site have been more difficult to describe with certainty. Our sequence comparison study between KCNQ2 and KCNQ3 led to the identification of KCNQ2 residues A181 and F168 as important determinants of sensitivity but does not demonstrate whether they directly contribute to binding (Wang et al., 2017). Based on the recent KCNQ1 cryo-EM structure, the predicted α-carbon distance between these two amino acid positions is ∼18 Å, while the end-to-end length of ICA73 is ∼12 Å, so it is unlikely that both amino acids contribute to a binding site (Sun and MacKinnon, 2017). More importantly, we have also demonstrated that ICA73 sensitivity persists in many A181 mutants (A181L and A181G; Wang et al., 2017). Only the more disruptive A181P substitution was found to diminish ICA73 effects. Other amino acids in the vicinity of A181 (E130, Y127, and R207) have also been suggested to play a role in a class of diclofenac derivatives that target the voltage sensor, and so a possible explanation for our findings is that the A181P substitution distorts the conformation of this region and weakens the affinity for ICA73 (leading to a faster dissociation rate as reported here), rather than making essential direct contacts with the drug. Although the effects of mutating F168 are more prominent, leading to complete loss of ICA73 sensitivity, it is more distant from this cluster of residues and has also been suggested to influence stability of the activated voltage sensor (Miceli et al., 2013). Thus, mutation of F168 may have indirect effects on voltage sensor activation that prevent ICA73 binding or effects. Further functional

and structural studies of the mechanisms of voltage sensor–targeted KCNQ openers will be required to describe the binding site of these compounds in more detail.

In summary, our study illustrates critical mechanistic differences between pore- and voltage sensor–targeted activators. These findings compliment previous structure–function experiments that delineate different structural requirements for sensitivity to these different drugs and also reveal important details related to drug binding to specific channel states.

Acknowledgments

This study was funded by Canadian Institutes of Health Research operating grant MOP 142482. C.K. Wang was supported by a Canadian Institutes of Health Research CGS-M graduate award. H.T. Kurata was supported by a Canadian Institutes of Health Research New Investigator Award and the Alberta Diabetes Institute.

The authors declare no competing financial interests.

Author contributions: C.K. Wang, S.M. Lamothe, and H.T. Kurata designed the experiments. C.K. Wang, S.M. Lamothe, A.W. Wang, and R.Y. Yang performed experiments. C.K. Wang, S.M. Lamothe, and H.T. Kurata analyzed data. C.K. Wang and H.T. Kurata wrote the manuscript. All authors provided edits and approved the final version of the manuscript.

Kenton J. Swartz served as editor.

Submitted: 16 March 2018
Revised: 24 July 2018
Accepted: 11 October 2018

References

Adams, P.R., and D.A. Brown. 1980. Luteinizing hormone-releasing factor and muscarinic agonists act on the same voltage-sensitive K+-current in bullfrog sympathetic neurones. *Br. J. Pharmacol.* 68:353–355. https://doi.org/10.1111/j.1476-5381.1980.tb14547.x

Barrese, V., J.B. Stott, and I.A. Greenwood. 2018. KCNQ-encoded potassium channels as therapeutic targets. *Annu. Rev. Pharmacol. Toxicol.* 58:625–648.

Bentzen, B.H., N. Schmitt, K. Calloe, W. Dalby Brown, M. Grunnet, and S.P. Olesen. 2006. The acrylamide (S)-1 differentially affects Kv7 (KCNQ) potassium channels. *Neuropharmacology.* 51:1068–1077. https://doi.org/10.1016/j.neuropharm.2006.07.001

Biervert, C., B.C. Schroeder, C. Kubisch, S.F. Berkovic, P. Propping, T.J. Jentsch, and O.K. Steinlein. 1998. A potassium channel mutation in neonatal human epilepsy. *Science.* 279:403–406. https://doi.org/10.1126/science.279.5349.403

Blom, S.M., N. Schmitt, and H.S. Jensen. 2010. Differential effects of ICA-27243 on cloned K(V)7 channels. *Pharmacology.* 86:174–181. https://doi.org/10.1159/000317525

Brown, D.A., and P.R. Adams. 1980. Muscarinic suppression of a novel voltage-sensitive K+ current in a vertebrate neurone. *Nature.* 283:673–676. https://doi.org/10.1038/283673a0

Brown, D.A., S.A. Hughes, S.J. Marsh, and A. Tinker. 2007. Regulation of M(Kv7.2/7.3) channels in neurons by PIP(2) and products of PIP(2) hydrolysis: Significance for receptor-mediated inhibition. *J. Physiol.* 582:917–925. https://doi.org/10.1113/jphysiol.2007.132498

Brueggemann, L.I., J.M. Haick, L.L. Cribbs, and K.L. Byron. 2014. Differential activation of vascular smooth muscle Kv7.4, Kv7.5, and Kv7.4/7.5 channels by ML213 and ICA-069673. *Mol. Pharmacol.* 86:330–341. https://doi.org/10.1124/mol.114.093799

Charlier, C., N.A. Singh, S.G. Ryan, T.B. Lewis, B.E. Reus, R.J. Leach, and M. Leppert. 1998. A pore mutation in a novel KQT-like potassium channel gene in an idiopathic epilepsy family. *Nat. Genet.* 18:53–55. https://doi.org/10.1038/ng0198-53

Gao, Z., T. Zhang, M. Wu, Q. Xiong, H. Sun, Y. Zhang, L. Zu, W. Wang, and M. Li. 2010. Isoform-specific prolongation of Kv7 (KCNQ) potassium channel opening mediated by new molecular determinants for drug-channel interactions. *J. Biol. Chem.* 285:28322–28332. https://doi.org/10.1074/jbc.M110.116392

Hernandez, C.C., O. Zaika, G.P. Tolstykh, and M.S. Shapiro. 2008. Regulation of neural KCNQ channels: Signalling pathways, structural motifs and functional implications. *J. Physiol.* 586:1811–1821. https://doi.org/10.1113/jphysiol.2007.148304

Kalappa, B.I., H. Soh, K.M. Duignan, T. Furuya, S. Edwards, A.V. Tzingounis, and T. Tzounopoulos. 2015. Potent KCNQ2/3-specific channel activator suppresses in vivo epileptic activity and prevents the development of tinnitus. *J. Neurosci.* 35:8829–8842. https://doi.org/10.1523/JNEUROSCI.5176-14.2015

Kharkovets, T., K. Dedek, H. Maier, M. Schweizer, D. Khimich, R. Nouvian, V. Vardanyan, R. Leuwer, T. Moser, and T.J. Jentsch. 2006. Mice with altered KCNQ4 K+ channels implicate sensory outer hair cells in human progressive deafness. *EMBO J.* 25:642–652. https://doi.org/10.1038/sj.emboj.7600951

Kim, R.Y., M.C. Yau, J.D. Galpin, G. Seebohm, C.A. Ahern, S.A. Pless, and H.T. Kurata. 2015. Atomic basis for therapeutic activation of neuronal potassium channels. *Nat. Commun.* 6:8116. https://doi.org/10.1038/ncomms9116

Kim, R.Y., S.A. Pless, and H.T. Kurata. 2017. PIP2 mediates functional coupling and pharmacology of neuronal KCNQ channels. *Proc. Natl. Acad. Sci. USA.* 114:E9702–E9711. https://doi.org/10.1073/pnas.1705802114

Kubisch, C., B.C. Schroeder, T. Friedrich, B. Lütjohann, A. El-Amraoui, S. Marlin, C. Petit, and T.J. Jentsch. 1999. KCNQ4, a novel potassium channel expressed in sensory outer hair cells, is mutated in dominant deafness. *Cell.* 96:437–446. https://doi.org/10.1016/S0092-8674(00)80556-5

Kumar, M., N. Reed, R. Liu, E. Aizenman, P. Wipf, and T. Tzounopoulos. 2016. Synthesis and evaluation of potent KCNQ2/3-specific channel activators. *Mol. Pharmacol.* 89:667–677. https://doi.org/10.1124/mol.115.103200

Lange, W., J. Geissendörfer, A. Schenzer, J. Grötzinger, G. Seebohm, T. Friedrich, and M. Schwake. 2009. Refinement of the binding site and mode of action of the anticonvulsant Retigabine on KCNQ K+ channels. *Mol. Pharmacol.* 75:272–280. https://doi.org/10.1124/mol.108.052282

Li, P., Z. Chen, H. Xu, H. Sun, H. Li, H. Liu, H. Yang, Z. Gao, H. Jiang, and M. Li. 2013. The gating charge pathway of an epilepsy-associated potassium channel accommodates chemical ligands. *Cell Res.* 23:1106–1118. https://doi.org/10.1038/cr.2013.82

Mackie, A.R., and K.L. Byron. 2008. Cardiovascular KCNQ (Kv7) potassium channels: Physiological regulators and new targets for therapeutic intervention. *Mol. Pharmacol.* 74:1171–1179. https://doi.org/10.1124/mol.108.049825

Main, M.J., J.E. Cryan, J.R. Dupere, B. Cox, J.J. Clare, and S.A. Burbidge. 2000. Modulation of KCNQ2/3 potassium channels by the novel anticonvulsant retigabine. *Mol. Pharmacol.* 58:253–262. https://doi.org/10.1124/mol.58.2.253

Martyn-St James, M., J. Glanville, R. McCool, S. Duffy, J. Cooper, P. Hugel, and P.W. Lane. 2012. The efficacy and safety of retigabine and other adjunctive treatments for refractory partial epilepsy: A systematic review and indirect comparison. *Seizure.* 21:665–678. https://doi.org/10.1016/j.seizure.2012.07.011

Miceli, F., M.V. Soldovieri, M. Martire, and M. Taglialatela. 2008. Molecular pharmacology and therapeutic potential of neuronal Kv7-modulating drugs. *Curr. Opin. Pharmacol.* 8:65–74. https://doi.org/10.1016/j.coph.2007.10.003

Miceli, F., M.R. Cilio, M. Taglialatela, and F. Bezanilla. 2009. Gating currents from neuronal K(V)7.4 channels: General features and correlation with the ionic conductance. *Channels (Austin).* 3:274–283. https://doi.org/10.4161/chan.3.4.9477

Miceli, F., M.V. Soldovieri, P. Ambrosino, V. Barrese, M. Migliore, M.R. Cilio, and M. Taglialatela. 2013. Genotype-phenotype correlations in neonatal epilepsies caused by mutations in the voltage sensor of K(v)7.2 potassium channel subunits. *Proc. Natl. Acad. Sci. USA.* 110:4386–4391. https://doi.org/10.1073/pnas.1216867110

Miceli, F., M.V. Soldovieri, P. Ambrosino, L. Manocchio, A. Medoro, I. Mosca, and M. Taglialatela. 2018. Pharmacological targeting of neuronal Kv7.2/3 channels: A focus on chemotypes and receptor sites. *Curr. Med. Chem.* 25:2637–2660.

Osteen, J.D., R. Barro-Soria, S. Robey, K.J. Sampson, R.S. Kass, and H.P. Larsson. 2012. Allosteric gating mechanism underlies the flexible gating of

KCNQ1 potassium channels. *Proc. Natl. Acad. Sci. USA.* 109:7103–7108. https://doi.org/10.1073/pnas.1201582109

Padilla, K., A.D. Wickenden, A.C. Gerlach, and K. McCormack. 2009. The KCNQ2/3 selective channel opener ICA-27243 binds to a novel voltage-sensor domain site. *Neurosci. Lett.* 465:138–142. https://doi.org/10.1016/j.neulet.2009.08.071

Peretz, A., L. Pell, Y. Gofman, Y. Haitin, L. Shamgar, E. Patrich, P. Kornilov, O. Gourgy-Hacohen, N. Ben-Tal, and B. Attali. 2010. Targeting the voltage sensor of Kv7.2 voltage-gated K+ channels with a new gating-modifier. *Proc. Natl. Acad. Sci. USA.* 107:15637–15642. https://doi.org/10.1073/pnas.0911294107

Ragsdale, D.S., J.C. McPhee, T. Scheuer, and W.A. Catterall. 1994. Molecular determinants of state-dependent block of Na+ channels by local anesthetics. *Science.* 265:1724–1728. https://doi.org/10.1126/science.8085162

Schenzer, A., T. Friedrich, M. Pusch, P. Saftig, T.J. Jentsch, J. Grötzinger, and M. Schwake. 2005. Molecular determinants of KCNQ (Kv7) K+ channel sensitivity to the anticonvulsant retigabine. *J. Neurosci.* 25:5051–5060. https://doi.org/10.1523/JNEUROSCI.0128-05.2005

Singh, N.A., C. Charlier, D. Stauffer, B.R. DuPont, R.J. Leach, R. Melis, G.M. Ronen, I. Bjerre, T. Quattlebaum, J.V. Murphy, et al. 1998. A novel potassium channel gene, KCNQ2, is mutated in an inherited epilepsy of newborns. *Nat. Genet.* 18:25–29. https://doi.org/10.1038/ng0198-25

Suh, B.C., and B. Hille. 2007. Regulation of KCNQ channels by manipulation of phosphoinositides. *J. Physiol.* 582:911–916. https://doi.org/10.1113/jphysiol.2007.132647

Suh, B.C., T. Inoue, T. Meyer, and B. Hille. 2006. Rapid chemically induced changes of PtdIns(4,5)P2 gate KCNQ ion channels. *Science.* 314:1454–1457. https://doi.org/10.1126/science.1131163

Sun, J., and R. MacKinnon. 2017. Cryo-EM structure of a KCNQ1/CaM complex reveals insights into congenital long QT syndrome. *Cell.* 169:1042–1050.e9. https://doi.org/10.1016/j.cell.2017.05.019

Vicente-Baz, J., J.A. Lopez-Garcia, and I. Rivera-Arconada. 2016. Effects of novel subtype selective M-current activators on spinal reflexes in vitro: Comparison with retigabine. *Neuropharmacology.* 109:131–138. https://doi.org/10.1016/j.neuropharm.2016.05.025

Wainger, B.J., E. Kiskinis, C. Mellin, O. Wiskow, S.S. Han, J. Sandoe, N.P. Perez, L.A. Williams, S. Lee, G. Boulting, et al. 2014. Intrinsic membrane hyperexcitability of amyotrophic lateral sclerosis patient-derived motor neurons. *Cell Reports.* 7:1–11. https://doi.org/10.1016/j.celrep.2014.03.019

Wang, A.W., R. Yang, and H.T. Kurata. 2017. Sequence determinants of subtype-specific actions of KCNQ channel openers. *J. Physiol.* 595:663–676. https://doi.org/10.1113/JP272762

Wang, A.W., M.C. Yau, C.K. Wang, N. Sharmin, R.Y. Yang, S.A. Pless, and H.T. Kurata. 2018. Four drug-sensitive subunits are required for maximal effect of a voltage sensor-targeted KCNQ opener. *J. Gen. Physiol.* 150:1432–1443. https://doi.org/10.1085/jgp.201812014 30166313

Wickenden, A.D., W. Yu, A. Zou, T. Jegla, and P.K. Wagoner. 2000. Retigabine, a novel anti-convulsant, enhances activation of KCNQ2/Q3 potassium channels. *Mol. Pharmacol.* 58:591–600. https://doi.org/10.1124/mol.58.3.591

Wickenden, A.D., J.L. Krajewski, B. London, P.K. Wagoner, W.A. Wilson, S. Clark, R. Roeloffs, G. McNaughton-Smith, and G.C. Rigdon. 2008. N-(6-chloro-pyridin-3-yl)-3,4-difluoro-benzamide (ICA-27243): A novel, selective KCNQ2/Q3 potassium channel activator. *Mol. Pharmacol.* 73:977–986. https://doi.org/10.1124/mol.107.043216

Wuttke, T.V., G. Seebohm, S. Bail, S. Maljevic, and H. Lerche. 2005. The new anticonvulsant retigabine favors voltage-dependent opening of the Kv7.2 (KCNQ2) channel by binding to its activation gate. *Mol. Pharmacol.* 67:1009–1017. https://doi.org/10.1124/mol.104.010793

Xiong, Q., H. Sun, and M. Li. 2007. Zinc pyrithione-mediated activation of voltage-gated KCNQ potassium channels rescues epileptogenic mutants. *Nat. Chem. Biol.* 3:287–296. https://doi.org/10.1038/nchembio874

Xiong, Q., Z. Gao, W. Wang, and M. Li. 2008. Activation of Kv7 (KCNQ) voltage-gated potassium channels by synthetic compounds. *Trends Pharmacol. Sci.* 29:99–107. https://doi.org/10.1016/j.tips.2007.11.010

Xu, W., Y. Wu, Y. Bi, L. Tan, Y. Gan, and K. Wang. 2010. Activation of voltage-gated KCNQ/Kv7 channels by anticonvulsant retigabine attenuates mechanical allodynia of inflammatory temporomandibular joint in rats. *Mol. Pain.* 6:49. https://doi.org/10.1186/1744-8069-6-49

Yau, M.C., R.Y. Kim, C.K. Wang, J. Li, T. Ammar, R.Y. Yang, S.A. Pless, and H.T. Kurata. 2018. One drug-sensitive subunit is sufficient for a near-maximal retigabine effect in KCNQ channels. *J. Gen. Physiol.* 150:1421–1431. https://doi.org/10.1085/jgp.201812013 30166314

Yu, H., M. Wu, S.D. Townsend, B. Zou, S. Long, J.S. Daniels, O.B. McManus, M. Li, C.W. Lindsley, and C.R. Hopkins. 2011. Discovery, synthesis, and structure activity relationship of a series of N-Aryl- bicyclo[2.2.1]heptane-2-carboxamides: Characterization of ML213 as a novel KCNQ2 and KCNQ4 potassium channel opener. *ACS Chem. Neurosci.* 2:572–577. https://doi.org/10.1021/cn200065b

Zhang, R.S., J.D. Wright, S.A. Pless, J.J. Nunez, R.Y. Kim, J.B. Li, R. Yang, C.A. Ahern, and H.T. Kurata. 2015. A conserved residue cluster that governs kinetics of ATP-dependent gating of Kir6.2 potassium channels. *J. Biol. Chem.* 290:15450–15461. https://doi.org/10.1074/jbc.M114.631960